Natural frequency of a composite girder with corrugated steel web

* Jiho Moon,[1] Hee-Jung Ko,[2] Ik Hyun Sung[3], and Hak-Eun Lee[4]

[1), 2, 4)] *School of Civil, Environmental & Architectural Engineering, Korea University, Seoul, Republic of Korea*
[3)] *Department of Civil Engineering, Hanseo University, ChungNam, Republic of Korea.*
[1)] *jmoon1979@gamil.com*

ABSTRACT

This paper presents the natural frequency of a composite girder with corrugated steel web (CGCSW). A corrugated steel web has negligible in-plane axial stiffness, due to the unique characteristic of corrugated steel webs, which is called the accordion effect. Thus, the corrugated steel web only resists shear force. Further, the shear buckling resistance and out-of-plane stiffness of the web can be enhanced by using a corrugated steel web, since the inclined panels serve as transverse stiffeners. To take these advantages, the corrugated steel web has been used as an alternative to the conventional pre-stressed concrete girder. However, studies about the dynamic characteristics, such as the natural frequency of a CGCSW, have not been sufficiently reported, and it is expected that the natural frequency of a CGCSW is different from that of a composite girder with flat web due to the unique characteristic of the corrugated steel web. In this study, the natural frequency of a CGCSW was investigated through a series of experimental studies and finite element analysis. An experimental study was conducted to evaluate the natural frequency of CGCSW. A parametric study was then performed to investigate the effect of the geometric characteristics of the corrugated steel web on the natural frequency of the CGCSW.

1. INTRODUCTION

Corrugated steel plates have been used as building and bridge components due to several advantages, such as high shear buckling resistance, and out-of-plane bending stiffness. In particular, the corrugated steel web has negligible bending capacity due to

---

[1)] Research Professor
[2)] Ph. D. Candidate
[3)] Professor
[4)] Professor
Note: Copied from the manuscript submitted to "Steel and Composite Structures, An International Journal" for presentation at ASEM13 Congress

the accordion effect. As a result, a corrugated steel web carries only shear forces, and the flanges and concrete slab carry the axial and bending normal stresses. Thus, the efficiency of pre-stressing can be enhanced by using a corrugated steel web instead of a conventional flat web. To take advantage of these factors, the composite girder with corrugated steel web (CGCSW) has been used in France, Japan, and South Korea as an alternative to the conventional pre-stressed concrete bridge. Further, the use of the corrugated steel web provides high fatigue resistance, by minimization of the welding process, and can overcome the disadvantages of conventional stiffened flat webs such as web instability due to bending normal stress (Ibrahim *et al.* 2006, Abbas *et al.* 2007).

A typical composite girder with corrugated steel web (CGCSW) is shown in Fig. 1. The x, y, and z axes shown in Fig. 1 are the global coordinates used in this study. The corrugated steel web could have a sinusoidal or trapezoidal shape, and only trapezoidal corrugated steel webs are considered in this study. The trapezoidal corrugated steel web is composed of a series of plane and inclined sub-panels, as shown in Fig. 1, where a is the length of the flat panel, c is the length of the inclined panel, b is the projection length of the inclined panel, θ is the corrugation angle, t_w is the thickness of the corrugated webs, and d is the maximum depth of corrugation.
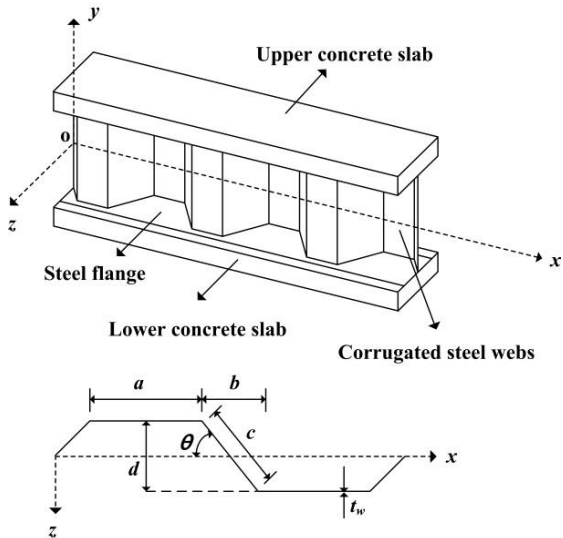

Fig. 1 Composite girder with corrugated steel web (CGCSW) and corrugation profiles.

Research on the corrugated steel web was initiated by Easley and McFarland (1969). Since then, numerous theoretical and experimental researches on the behavior of corrugated steel webs have been studied (Yoda *et al.* 1994, Luo & Edlund 1996, Elgaaly *et al.* 1997, Chan *et al.* 2002, Ibrahim *et al.* 2006, Abbas *et al.* 2007, Yi *et al.* 2008, Biancolini *et al.* 2009, Kiymaz *et al.* 2010, Moon *et al.* 2009a, 2009b, 2013). However, studies about dynamic characteristics, such as the natural frequency of a CGCSW, have rarely been reported, even if the natural frequency is essential information for dynamic analysis. It is also expected that the natural frequency of a CGCSW is different from that of a composite girder with flat web due to several unique characteristics of the corrugated steel web.

In this study, the natural frequency of a CGCSW was investigated through a series of

experimental programs and finite element analysis. A large scale specimen of CGCSW was constructed and tested to evaluate the natural frequency of the CGCSW. A series of parametric studies was then conducted to investigate the effect of geometrical characteristics of the corrugated steel web on the natural frequency.

2. EXPERIMENTAL STUDY

2.1 Description of experimental program

A large scale test specimen of composite girder with corrugated steel web (CGCSW) was constructed. Figure 2 (a) shows the dimensions of the test specimen. The span length of the specimen was 10.3 m. The width of the flat panel a was 180 mm, the projection width of the inclined panel b was 140 mm, the maximum depth of corrugation d was 100 mm, the thickness of the corrugated steel web t_w was 8 mm, and the height of the corrugated steel web h_w was taken as 1000 mm. As a result, a/h_w was 0.18, θ was 35.5°, and the length reduction factor η, which is defined as $(a+b)/(a+c)$, was 0.91. These values were selected to have similar corrugation profiles to existing CGCSW bridges. The steel flange was attached to the top and bottom of the corrugated steel web, and connected to the upper and lower concrete slab with shear studs to ensure composite action of the CGCSW. The width and thickness of the top and bottom steel flange were 300 mm and 15 mm, respectively. The width and height of the upper and lower concrete slab were 500 mm and 250 mm, respectively. Four bracings were installed, to guarantee the safety for unexpected overturning of the test specimen, as shown in Fig. 2 (a). It should be noted that these bracings were not in contact with the test specimen.
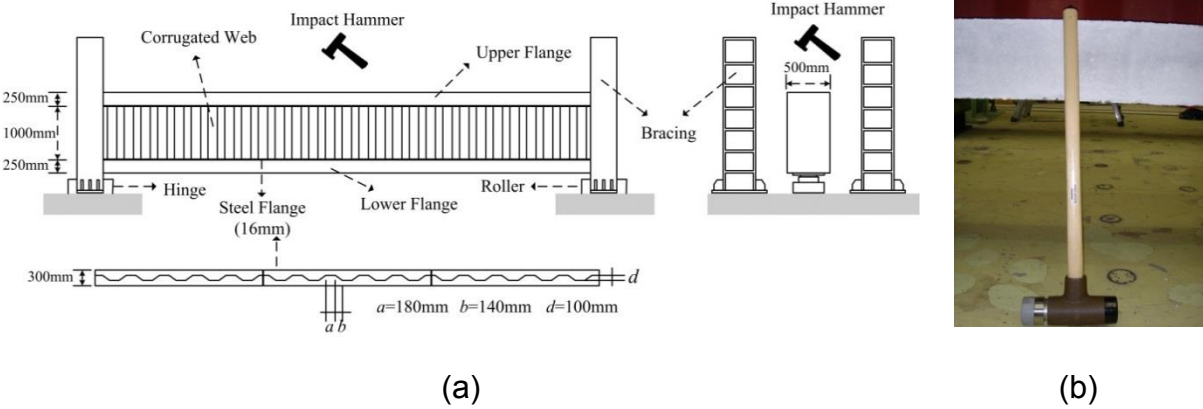

(a) (b)

Fig. 2 Test specimen and setup: (a) Dimensions of specimen; and (b) Impact hammer.

The impact hammer shown in Fig. 2 (b) was used to apply an impulsive load to the test specimen, where the mass of the impact hammer was 5.5 kg. An impact was added on the center of the top concrete slab in the in-plane direction, and acceleration data was obtained with the time interval of 0.004 sec. Then, the natural frequency of the CGCSW was evaluated from Fast Fourier Transform (FFT) analysis with acceleration data obtained from free vibration test. To ensure the reoccurrence of the natural frequency, the same test was conducted more than 10 times. Eight servo accelerometers were used to measure the acceleration generated by impulsive load,

and the arrangement of accelerometers is shown in Fig. 3, where the vibration frequency ranges of servo accelerometers used in this study varies from 1 Hz to 250 Hz.
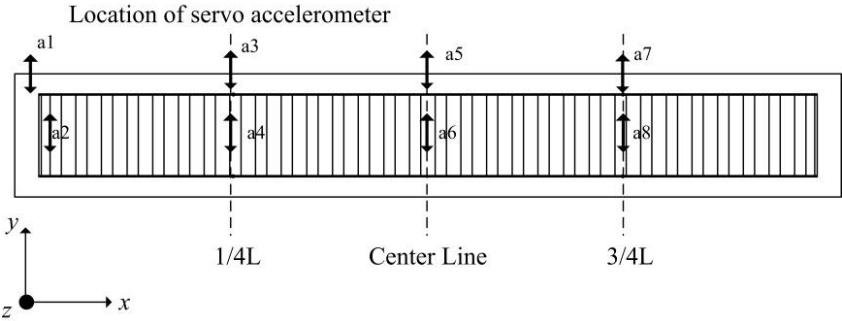

Fig. 3 Arrangement of servo accelerometers.

The CGCSW is usually pre-stressed, by using internal tendons to control the cracks in a concrete slab in the service load level. Further, external tendons are sometimes used, if necessary. In this study, the effect of internal and external tendon on the natural frequency of CGCSW was investigated, through a series of experimental studies. Table 1 shows the details of test specimens. The NT specimen served as the base model, and had no internal or external tendons. E0_I1 in Table 1 had only two internal tendons in the center of the lower concrete slab, where the jacking force was 208.53 kN, and the ratio of jacking force to ultimate tendon force was 0.8. It is noted that SWPC 7B tendon was used for both internal and external tendons, where the area and ultimate tendon force of SWPC 7B are 138.7 mm^2 and 260.8 kN, respectively. In the case of test specimens with external tendons (E1_I0 - E6_I0 in Table 1), the external tendons were installed on both sides of the test specimen, and the angle of external tendons varied from 3° to 11°, by changing the location of the end and center anchorages. The jacking forces of E1_I0-E6_I0 were determined to induce the in-plane bending moment of 107.9 kN·m at the center of the test specimens. The ratios of jacking force to ultimate tendon force of E1_I0 - E6_I0 varied from 0.54 to 0.88, as shown in Table 1.

Table 1 Details of test specimens.

Model	Internal tendon	External tendon	Angle (degree)	Jacking force (kN)	Jacking force/ ultimate tendon force
NT	x	x	N/A	N/A	N/A
E1_I0	x	o	8	229.12	0.88
E2_I0	x	o	10	175.03	0.67
E3_I0	x	o	11	141.90	0.54
E4_I0	x	o	3	227.36	0.87
E5_I0	x	o	5	173.17	0.66
E6_I0	x	o	7	140.04	0.54
E0_I1	o	x	0	208.54	0.80

2.2 Test results

Figure 4 shows the acceleration data obtained from the free vibration test and FFT analysis for a3, a4, and a8 accelerometers of the NT specimen shown in Table 1. The

FFT analysis results were almost identical to each other, regardless of the location of accelerometer, as shown in Fig. 4. In this study, the natural frequency of the test specimen was evaluated based on the acceleration data of a3 accelerometer for all specimens, since the variation of the natural frequency depending on the location of accelerometer was very small. As mentioned before, the same test was conducted more than 10 times for each case to ensure the reoccurrence of the natural frequency. Thus, the natural frequency of test specimens was determined by averaging the FFT results of a3 accelerometer for each case, and the results are summarized in Table 2
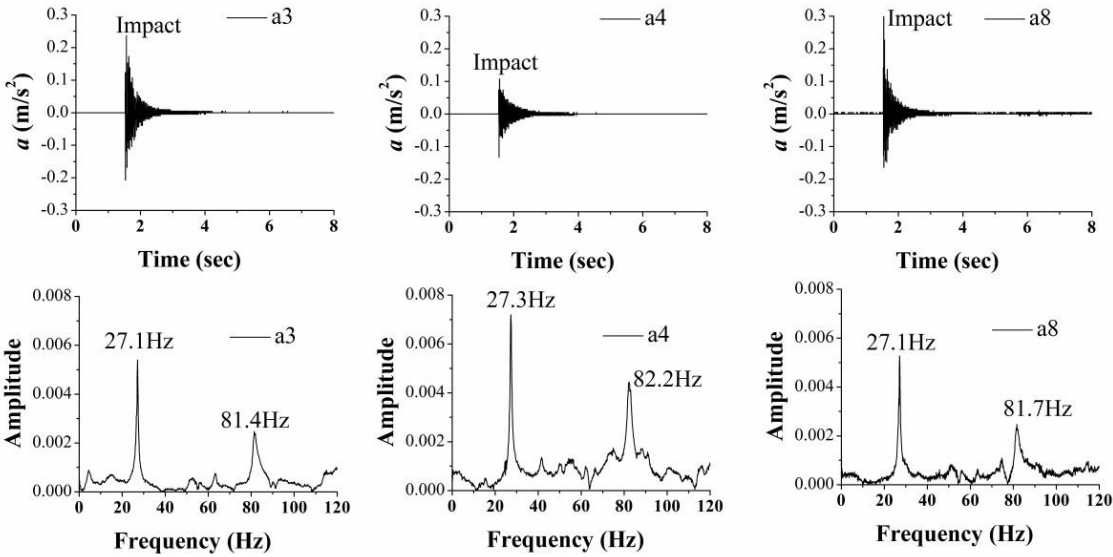

Fig. 4 Acceleration data vs. time and FFT analysis results for a3, a4 and a8 accelerometers (NT specimen).

Table 2 Summary of average natural frequency of test specimens.

Model	1st average natural frequency (Hz)	2nd average natural frequency (Hz)
NT	27.1	81.4
E1I0	27.3	82.2
E2I0	27.2	82.4
E3I0	27.2	81.5
E4I0	27.3	82.4
E5I0	27.2	82.4
E6I0	27.2	82.2
E0I1	27.1	81.8

From Table 2, it was found that the 1st and 2nd average natural frequencies of test specimens were almost identical to each other regardless of the existence of internal or external tendons. The maximum discrepancy was 1% for both 1st and 2nd average natural frequency, as shown in Table 2. This is because the mass of the internal and external tendon was very small compared with that of the test specimens. Further, the applied moment and axial force induced by internal or external tendons were also small compared with the bending and axial load capacity of the specimen without internal or external tendon. Thus, effect of internal and external tendons on the natural frequency

was insignificant.

3. PARAMETRIC STUDY

A series of parametric studies was conducted to investigate the effect of the geometric characteristics of the corrugated steel web on the natural frequency of the CGCSW by using the three dimensional finite element model. Finite element analysis was performed by using a general purpose structural analysis program ABAQUS (2009). An 8-node solid element, 4-node shell element, and 2-node truss element were used to model the concrete slab, steel sections, and reinforcing bar, respectively. The reinforcing bar was embedded into the concrete slab by using the EMBEDED option in ABAUQS (2009), and it is assumed that the reinforcing bar and concrete were perfectly bonded. The concrete slabs and steel flanges were also perfectly bonded by using the TIE option in ABAQUS (2009), since the concrete slabs and steel flanges were connected by shear studs, and the slip is negligible for small loading, such as the impulsive loading induced by impact hammer used in this study for the free vibration test. The materials were assumed as linear elastic. The elastic modulus of concrete and steel were taken as 28,000 MPa and 210,000 MPa, respectively. The mass density of the concrete and steel were assumed as 2,500 kg/m^3 and 7,850 kg/m^3, respectively.

Table 3 Profiles of the finite element models for parametric study.

L (mm)	b (mm)	t (mm)	b_f (mm)	t_f (mm)	h_w (mm)	t_w (mm)	a (mm)	b (mm)	d (mm)	θ (°)
10,000	500	250	250	15	1000	8	180	140	25-120	10.1-40.6

Table 3 shows the profiles of the analysis model for the parametric study. The analysis model was selected similar to the test specimen. The length of the model was 10 m, width of the concrete slab b was 500 mm, and the thickness of the concrete slab t was 250 mm. The width and thickness of steel flange (b_f and t_f) were 250 mm and 15 mm, respectively. For the corrugated steel webs, the width of flat panel a, and the projection length of inclined panel b were 180 mm and 140 mm, respectively. The maximum corrugation depth d is the main parameter, and d varied from 25 to 120. As a result, the corrugation angle θ ranged from 10.1° to 40.6°. Stirrups were installed in the upper and lower concrete slabs with a spacing of 125 mm, where D10 bar was used (the area of D10 bar is 71.33 mm^2). Four longitudinal reinforcing bars were also installed in the concrete slabs, where D17 bar was used (the area of D17 is 198.6 mm^2). The resulting longitudinal reinforcement ratio was 0.64 %. Hinge and roller supports were assumed at the center of the left and right ends of the analysis model. Displacements in the x, y, and z direction were restrained for the hinge support, while displacements in the y and z axes were constrained for roller support. In addition, rotation about the x axis was constrained for both centers of the right and left ends. Finally, displacements in the y, and z directions of the right and left ends were restrained to prevent distortion of the cross section.

The results of parametric study are shown in Fig. 5. In Fig. 5, x and y axes represent the corrugation angle and normalized natural frequency, respectively. It is noted that the natural frequency was normalized with the results of the analysis model with θ =

10.1° (the smallest θ among the analysis models). From Fig. 5 (a), it can be seen that the in-plane natural frequency of CGCSW slightly decreased with increasing corrugation angle θ. The natural frequency was approximately 2.5% decreased with increasing θ from 10.1° to 40.6°. This is because the in-plane bending stiffness of CGCSW remains constant, while the total mass of CGCSW slightly increases with increasing θ. The effect of the corrugated steel web on the in-plane bending stiffness is usually ignored, because it is assumed that the corrugated steel web has negligible axial stiffness due to the accordion effect. Thus, the bending stiffness is all the same for the analysis models, while the total mass of the CGCSW slightly increases with increasing θ, since the unfolded length of the corrugated steel web increases with increasing θ. For example, the total mass of CGCSW increases 1.1% with increasing θ from 10.1° to 40.6° for the analysis models used in this study.
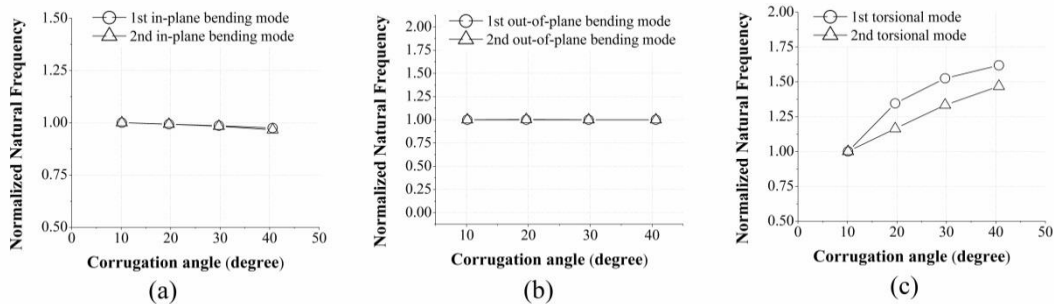

Fig. 5 Natural frequency vs. corrugation angle: (a) In-plane bending mode; (b) Out-of-plane bending mode; and (c) Torsional mode.
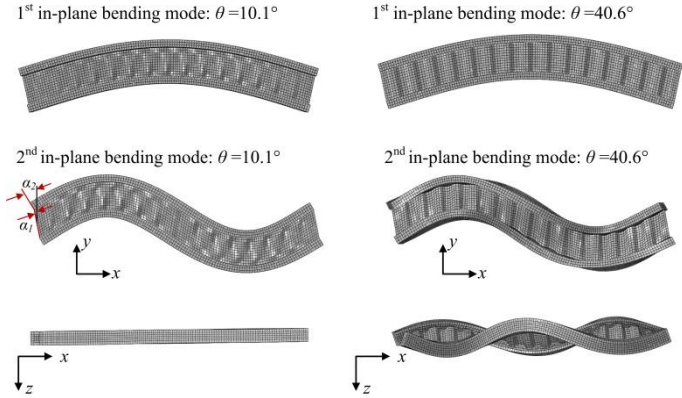

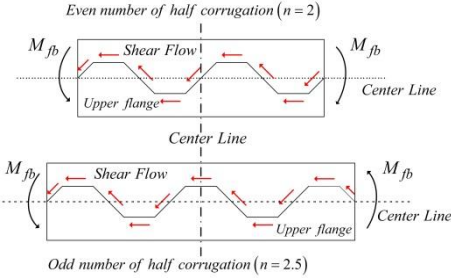Fig. 6 In-plane bending mode of analysis models (θ=10.1, and 40.6°).

Fig. 7 Flange bending mechanism of I-girder with corrugated webs

Figure 6 shows the 1st and 2nd in-plane bending modes of the analysis model with θ = 10.1° and 40.6°. It can be seen that the 1st in-plane bending mode is similar for the models with 10.1° and 40.6°, and negligible out-of-plane displacements of the concrete slabs were observed for both models. However, for the 2nd in-plane bending mode, the out-of-plane displacements of the concrete slabs of the analysis model with θ = 40.6°

were very large, as shown in Fig. 6. These out-of-plane displacements are generated by the shear flow acting along the edge of the corrugated steel web. Figure 7 shows the flange bending moment mechanism of an I-girder with corrugated steel web (Abbas *et al.* 2007, and Moon *et al.* 2013). The shear flow acting along the corrugated steel web generates flange bending moment M_f, as shown in Fig. 7, and the magnitude of M_f increases with increasing corrugation depth *d* (or corrugation angle *θ*). Thus, for the analysis model with *θ* = 40.6°, the in-plane bending mode was combined with the torsional mode. It was also found that the rotational angle of the corrugated steel web (*α1* in Fig. 6) was considerably different from that of the concrete slab (*α2* in Fig. 6), as shown in Fig. 6. These results imply that shear deformation of the corrugated steel web affects *α1*. Machindamrong *et al.* (2004) indicated that the effect of shear deformation of the corrugated steel web on the in-plane deflection is considerable. A similar result was observed from the deformation shape of the in-plane bending mode shown in Fig. 6, and the effect of shear deformation was higher for the 2nd in-plane bending mode comparing with the 1st mode.

In the case of the out-of-plane bending natural frequency of CGCSW, the natural frequency is almost identical, regardless of *θ*, as shown in Fig. 5 (b). This is because the out-of-plane stiffness of the corrugated steel web and total mass of the CGCSW slightly increase at the same time with increasing *θ* (or corrugation depth *d*). The corrugated steel web is eccentrically attached with the maximum corrugation depth d to the steel flanges and concrete slabs (refer Fig. 1). The out-of-plane bending stiffness of the corrugated steel web about the center of the steel flanges and concrete slabs is equal to $(h_w t_w^3)/12+(h_w t_w)d^2_{avg}/4$, where d_{avg} is the average corrugation depth (Moon *et al.* 2013). Thus, the out-of-plane bending stiffness increases with increasing *d*. For example, the out-of-plane bending stiffness of the analysis models increases approximately 2.2% with increasing *θ* from 10.1° to 40.6°.
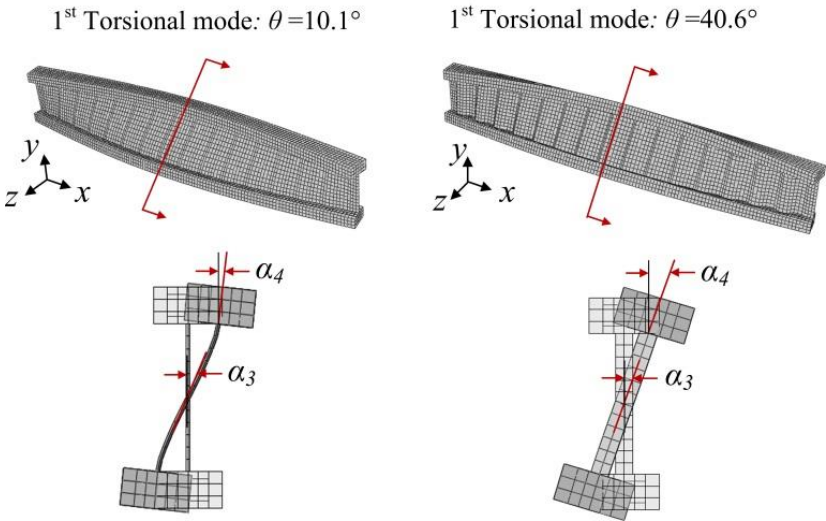

Fig. 8 Torsional mode of analysis models (*θ*=10.1, and 40.6°).

Figure 5 (c) shows the variation of the torsional natural frequency of the CGCSW in *θ*. The torsional natural frequency increases significantly with increasing *θ*. Figure 8

represents the torsional mode of the analysis models with θ = 10.1° and 40.6°. For the analysis model with θ = 10.1°, the twisting angle of the corrugated steel web ($\alpha3$ in Fig. 8) was larger than the twisting angle of the concrete slab ($\alpha4$ in Fig. 8), as shown in Fig. 8. This implies that the concrete slabs were not fully twisted, since the bending stiffness of the corrugated steel web itself about the x axis is too small to transfer the full twisting moment to the concrete slabs. The bending stiffness of the corrugated steel web about the x axis is a function of the corrugation depth d, and the stiffness increases with increasing d (or θ). For the model with θ = 40.6°, the concrete slabs were clearly twisted with almost the same torsional angle of the corrugated steel web. Thus, the torsional natural frequency of the CGCSW increases with increasing θ.

4. CONCLUSIONS

This study investigated the natural frequency of a composite girder with corrugated steel web (CGCSW), through a series of tests and finite element analyses. A large scale test specimen was constructed and tested to evaluate the natural frequency of the CGCSW. The major parameter of the test was the effect of internal and external tendons on the natural frequency of the CGCSW. From the test results, it was found that neither the internal nor external tendons had significant effects on the natural frequency of the CGCSW. A parametric study was then conducted to evaluate the effect of corrugation profiles on the natural frequency of the CGCSW. From the analysis results, the following conclusions were made:

(1) The in-plane bending natural frequency slightly decreases with increasing corrugation angle, since the total mass of the CGCSW slightly increases, while the in-plane bending stiffness remains constant due to the accordion effect. Also, it was found that the in-plane bending mode was combined with the torsional mode when the corrugation angle is large, since the flange bending moment is considerable.

(2) The variation of out-of-plane bending natural frequency with the corrugation angle is negligible. This is because the total mass and out-of-plane bending stiffness of the CGCSW simultaneously increase with increasing the corrugation angle.

(3) The twisting angle of the concrete slabs and corrugated steel web were considerably different when the corrugation angle was small, since the bending stiffness of the corrugated steel web about x axis (Refer Fig. 8) is not sufficient. Therefore, the torsional natural frequency decreases with decreasing corrugation angle. Further, adequate corrugation depth should be provided to develop a uniform twisting angle throughout the section.

REFERENCES

ABAQUS (2009), *ABAQUS analysis user's manual version 6.9-2*, Dassault systemes Simulia Corp. Providence, RI, USA.

Abbas, H.H., Sause, R., and Driver, R.G. (2007) "Analysis of flange transverse bending of corrugated web I-girders under in-plane loads" *J. Struct. Eng. ASCE* **133(3)**, 347-355.

Biancolini, M.E., Brutti, C., and Porziani, S. (2009) "Analysis of corrugated board panels under compression load", *Steel. Compos. Struct.*, **9(1)**, 1-17.

Chan, C.L., Khalid, Y.A., Sahari, B.B., and Hamouda, A.M.S. (2002) "Finite element analysis of corrugated web beams under bending", *J. Constr. Steel. Res.*, **58**, 1391-1406.

Easley, J.T., and McFarland, D.E. (1969) "Buckling of light-gauge corrugated metal shear diaphragms" *J. Sruct. Div. ASCE*, **95(ST7**), 1497-1516.

Elgaaly, M., Seshadri, A., and Hamilton, R.W. (1997) "Bending strength of steel beams with corrugated webs" *J. Struct. Eng. ASCE*, **123(6)**, 772-782.

Ibrahim, S.A., El-Dakhakhni, W.W., and Elgaaly, M. (2006) "Behavior of bridge girder with corrugated webs under monotonic and cyclic loading" *Eng. Struct.*, **28**, 1941-1955.

Kiymaz, G., Coskun, E., Cosgun, C., and Seckin E. (2010) "Transverse load carrying capacity of sinusoidally corrugated steel web beams with web openings" *Steel. Compos. Struct.*, **10(1)**, 69-85.

Luo, R., and Edlund, B. (1996) "Shear capacity of plate girders with trapezoidally corrugated webs", *Thin Wall. Struct.*, **26**, 19-44.

Machimdarong, C., Watanabe, E., and Utsunomiya, T. (2004) "Analysis of corrugated steel web girders by an efficient beam bending theory" *Structural Eng./Earthquake Eng. JSCE*, **21(2)**,131s-142s.

Moon, J., Yi, J., Choi, B.H., and Lee, H.-E. (2009a) "Lateral-torsional buckling of I-girder with corrugated webs under uniform bending" *Thin Wall. Struct.*, **47**, 21-30.

Moon, J., Yi, J., Choi, B.H., and Lee, H.-E. (2009b) "Shear strength and design of trapezoidally corrugated steel webs" *J. Constr. Steel. Res.*, **65**, 1198-1205.

Moon, J., Lim, N.-M., and Lee, H.-E. (2013) "Moment gradient correction factor and inelastic flexural‒torsional buckling of I-girder with corrugated steel webs" *Thin Wall. Struct.*, **62**, 18-27.

Yi, J., Gil, H., Youm, K., and Lee, H.-E. (2008) "Interactive shear buckling of trapezoidally corrugated webs" *Eng. Struct.*, **30**, 1659-1666.

Yoda, T., Ohura, T., and Sekii, K. (1994) "Analysis of composite PC Box girders with corrugated steel webs", *The Proc. of 4th Int. conf. on short and medium span bridges*, 1107-15.